Effect of hysteretic damping and stiffness at unloading on response of ground during Earthquake

N. Yoshida
Tohoku Gakuin University, Japan

ABSTRACT: Although many stress-strain models used in the dynamic response analysis of ground employ Masing rule to build hysteresis curves from a skeleton curve, actual damping characteristics does not follow it. The difference between the hysteresis curves made by Masing rule and those obtained in the laboratory test becomes significant at large strains. A rule to build hysteresis curves that satisfy both damping characteristics and modulus at unloading point is presented. In order to use this method, modulus at unloading point is obtained from the dynamic deformation characteristics test result, and it is shown that this modulus can be expressed by a hyperbolic model with respect to strain, with minimum modulus. Finally a case study is conducted to examine the effect of hysteretic damping characteristics on the dynamic response. It is shown that hysteretic damping characteristics affect the dynamic response significantly. Moreover, in contrary of common sense, earthquake motion at ground surface is larger as hysteretic damping becomes larger.

1 INTRODUCTION

Since soil shows nonlinear behavior even at small strain, it is essential to consider it in the earthquake response analysis. In many constitutive models used for geo-material, stress-strain relationship is composed of skeleton curve under virgin loading and hysteresis curve under unloading and/or reloading process. On the other hand, strain dependent characteristics of soil under repeated loading such as earthquake is expressed as dynamic deformation characteristics or, so called, G-γ and h-γ relationships. Comparison of there two concept, it is usually recognized that G-γ and h-γ relationships corresponds to skeleton and hysteresis curves, respectively.

As shown in this expression, both stiffness and damping characteristics have been believed to be important factor. It looks obvious that larger damping suppress amplification of the earthquake motion toward the ground surface. However, the possibility appears during the 1995 Hyogoken-nambu (Kobe) earthquake that this simple concept may not be true at large earthquakes. Suetomi and Yoshida (1998) showed that deamplification of earthquake motion occurs if there is soft soil such as Holocene clay from the earthquake response analysis at Kobe city. It explained the damage ratio of wooded houses is smaller near the shore and how south (shore side) boundary of the seismic belt zone with severe earthquake motion of seismic intensity I_{JMA} is seven (maximum intensity) existed north of the one expected by theory. After that Suetomi et al. (2000) confirmed that the peak acceleration at the ground surface has upper boundary associated by the shear strength of the weakest layer. It indicates that amplification of the ground may be determined regardless to damping characteristics. It is, however, difficult to confirm it by numerical analysis because of the following reason.

The hysteresis curve is obtained from the skeleton curve by applying the Masing's rule in many constitutive models. It is convenient to handle or to develop computer codes because hysteresis no other information except the skeleton curve is enough in evaluating hysteresis curve. On the other hand, the Masing's rule does not hold in the actual soil. It can be easy recognized,

for example, that damping characteristics by Hardin and Drnevich (1972) do not coincide with the damping characteristics of hyperbolic model that they proposed as G-γ curve. In spite of this clear fact, many computer codes used Masing's rule because there is no good hysteresis model. It indicates that numerical analysis that change damping characteristics by keeping stiffness characteristics unchanged is impossible.

In order to overcome this shortage, the author had proposed a new hysteresis rule by which one can obtain damping characteristics that completely coincide with test result (Ishihara et al., 1985). This concept has been employed in several models (Iai et al., 1999; Railway Technical Research Institute, 1999). This model extended by employing piecewisely defined skeleton curve such as piecewise linear or Lagrangean interpolation, by which one can obtain stress-strain model that can fit G-γ and h-γ relationships perfectly (Yoshida et al., 1990).

The author then compared earthquake response of the ground by using both hyperbolic and Hardin-Drnevich models (Takeshima et al., 2003). Note that both models have identical skeleton curve and different damping characteristics. It was shown that not only strain dependent stiffness and damping characteristics but also stiffness at unloading may affect the response of the ground. In this paper, a new model is proposed in which stiffness at unload can be considered and effect of both damping characteristics and stiffness at unload is examined.

2 MODELING OF HYSTERESIS CURVE

The concept to build hysteresis curve that has damping characteristics arbitrary specified is shown in Figure 1 schematically (Ishihara et al., 1985), where τ and γ denote shear stiffness and shear strain, respectively, and the subscript R denotes unloading. Here, hysteresis curve should satisfy two requirements. The one is that if unload occurs at (τ_R γ_R), then it should pass axial symmetric point ($-\tau_R$ $-\gamma_R$). The other is that damping constant is to be equals to the specified value. We consider a fictitious skeleton curve by which above two conditions is satisfied if Masing's rule is employed to this fictitious skeleton curve. Since there is two conditions, mathematical that has more than two parameters can be used for the fictitious skeleton curve.

The simplest model that satisfy this condition is a hyperbolic model expressed as

$$\tau = \frac{G_0 \gamma}{1 + \gamma / \gamma_r} \tag{1}$$

where G_0 is shear modulus at unload and γ_r is a parameter. When we use this model, G_0 is replaced with elastic shear modulus G_{max}, and γ_r is evaluated from shear strength τ_f as $\gamma_r = \tau_f / G_{max}$. In the skeleton curve, the reference strain has physical meaning, but it does not have physical meaning but a mere parameter.

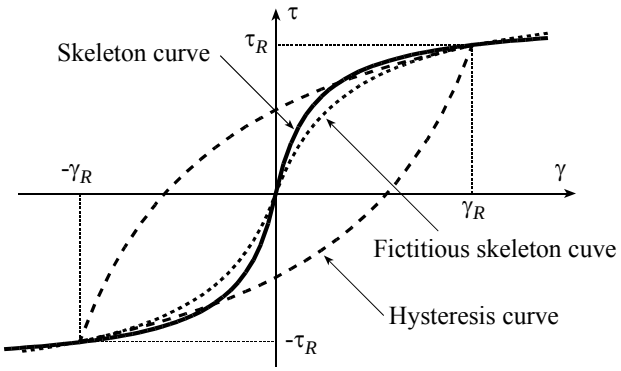

Figure 1. Hysteresis curve that developed from fictitious skeleton curve.

Since the damping ratio varies from zero to $2/\pi$, the theoretically maximum value, this model can be used under any damping ratio. In this sense, it is one of the most convenience and easy handling model although it has shortage that G_0 is used as a parameter.

If one wants to add an additional condition that, for example, shear modulus at unload is equal to elastic shear modulus, one needs a model that uses more than three parameters.

In this paper, we control shear modulus at unload in addition to strain dependent shear modulus and damping ratio, we needs a three-parameters model at minimum. A Ramberg-Osgood model is one of the relevant models, and frequently used model models that have been used in practice. This model is expressed as

$$\gamma = \frac{\tau}{G_0}\left\{1 + \alpha\tau^{\beta-1}\right\} \tag{2}$$

where α and β are parameters. If Masing's rule is applied, damping ratio yields

$$h = h_{max}\left(1 - G/G_0\right) \tag{3}$$

where h_{max} is a maximum damping ratio. Note that damping ratio is same as that proposed by Hardin & Drnevich (1972), which is the reason why this model has been used in practice as well as hyperbolic model. The relationship between h_{max} and model parameters is expressed as

$$h_{max} = \frac{2}{\pi}\frac{1-\beta}{1+\beta} \tag{4}$$

Since values of h, G and G_0 are known at the unloading point, h_{max} is evaluated from Eq. (3). The value of β is evaluated by substituting h_{max} into Eq. (4). Finally the value of α is computed from Eq. (2) by substituting these quantities. It is necessary to solve nonlinear equation in order to calculate parameters for hyperbolic model is used for hysteresis curve, but they are sequentially obtained in the Ramberg-Osgood model.

3 MODELING OF STIFFNESS AT UNLOAD

In many constitutive models, stiffness at unload is defined to be same as initial or elastic modulus, but it may change. In order to grasp strain dependency of stiffness at unload, stiffness at unload is read from stress-strain curve of the Toyoura sand with relative density D_r of 50 and 80 % and Holocene clay sampled at Tokyo. Here, the stiffness is evaluated by using several points after unloading. They are shown in Figure 2 as solid circles and G_0 with ordinary secant modulus G (with hollow circle). The solid line in the figure is a hyperbolic model

$$\frac{G}{G_{max}} = \frac{1}{1+\gamma/\gamma_r} \tag{5}$$

whose coefficient is chosen to fit the experiment. Here, it is noted that both Eq. (5) and Eq. (1) are identical. The evaluated values are summarized in
Table 1.

It is clearly seen that modulus at unload is not constant but depends on shear strain. These relationships are modeled into another hyperbolic model as

$$\frac{G_0}{G_{max}} = \frac{1 - G_{min}/G_{max}}{1+\gamma/\gamma_{r0}} + \frac{G_{min}}{G_{max}} \tag{6}$$

where G_{min} is the minimum stiffness at unload, and γ_{r0} is reference strain for stiffness at unload. Dotted line in Figure 2 is a fitted curve and agreement with test result is as good as ordinary G-γ curves. The evaluated values are shown in
Table 1. General tendencies of the curves are as follows:

1) γ_{r0} becomes greater as γ_r increases
2) G_{min}/G_{max} is larger for sand than that of clay

In the case of sand, two characteristics which are decrease of stiffness as excess porewater pressure generates and increase of stiffness by cyclic mobility seems key factors affecting the stiffness at unload. Since decrease of stiffness occurs at small strain where excess porewater generation is not expected occurs, another factor, possible a mere nonlinear behavior, also affects this

characteristics. Minimum stiffness is larger for sand with D_r=80 % than that of sand with D_r=50 %, which seems to come from the difference of cyclic mobility.

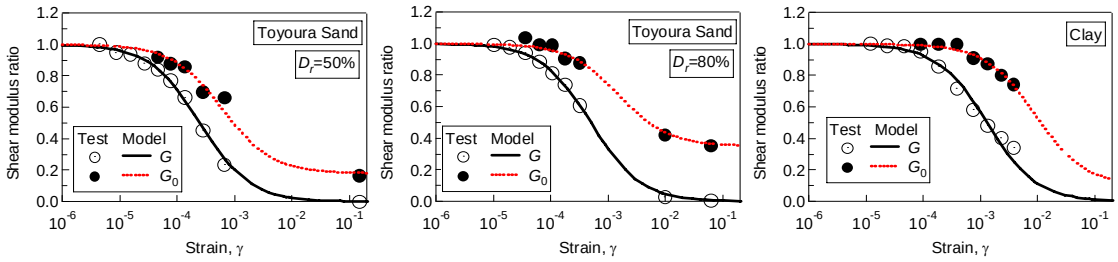

Figure 2. Shear modulus and stiffness at unload as a function with respect to strain

Table 1 Evaluated model parameters

Material	γ_r	γ_{r0}	G_{min}/G_{max}
Sand (D_r=50%)	0.00025	0.0006	0.18
Sand (D_r=80%)	0.0005	0.0015	0.35
Clay	0.0013	0.013	0.1

4 A CASE STUDY

The effects of hysteretic damping and stiffness at unload is examined through a numerical study. A ground in Tokyo city area (Sato et al., 1998) shown in
Figure 3 is used in this case study.

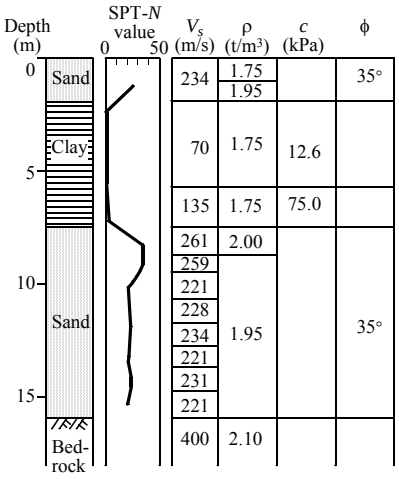

Figure 3. Soil profiles

4.1 *Soil profiles and material*

Dynamic deformation characteristics of this site are modeled into Hardin-Drnevich model by Sato et al. (1998). Model parameters are summarized in Table 2, dynamic deformation characteristics are shown in Figure 4 as H-D model (dashed line).

Three stress-strain models are used in this case study. All models have the same hyperbolic skeleton curve expressed as Eq. (1), but hysteresis curves are differently defined.

1) Hyperbolic model: ordinary hyperbolic model whose hysteresis loop is made by applying the Masing's rule. This model is referred as "Hyperbolic."
2) H-D model: damping characteristics is evaluated from Eq. (3). This model gives the same strain dependent shear modulus and damping characteristics proposed by Hardin and Drnevich (1972). Since the hyperbolic model is used for hyperbolic is used for the hyper-

bolic model, stiffness at unload cannot be controlled, but determined automatically. This model is referred as "H-D"

3) Same as "H-D", but hysteresis curve is made by means of R-O model. Therefore, stiffness at unload can also be controlled, and Eq. (6) is used to evaluate it. This model is referred as "H-D /w E". Note that both "H-D" and "H-D /w E" gives the same damping characteristics shown as H-D in Figure 4, and will be call H-D type model in the discussion, especially to compare with hyperbolic model which shows much larger damping.

Damping characteristics of the hyperbolic model is also shown in Figure 4. As well known, the hyperbolic model shows much larger damping at large strain than that of the H-D model, but damping at small strain is nearly the same for both models. Figure 5 compares stress-strain curve of three models for shear strain amplitude of 0.6 % and 4 %, respectively. Curves are quite different between hyperbolic model and two H-D type models, but that those by two H-D type models are similar to each other, which indicates that stiffness at unload may not be a key factor.

Table 2. Model parameters

Material	γ_r	h_{max}	γ_{r0}	G_{min}/G_{max}
Sand	8.63×10^{-4}	0.22	0.002	0.4
Clay	1.42×10^{-3}	0.22	0.013	0.1

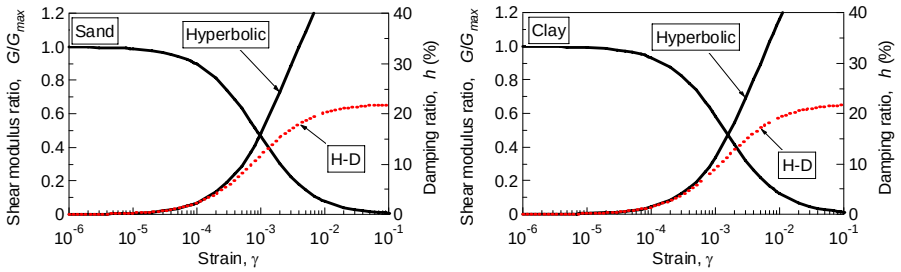

Figure 4. Dynamic deformation characteristics of sand and clay.

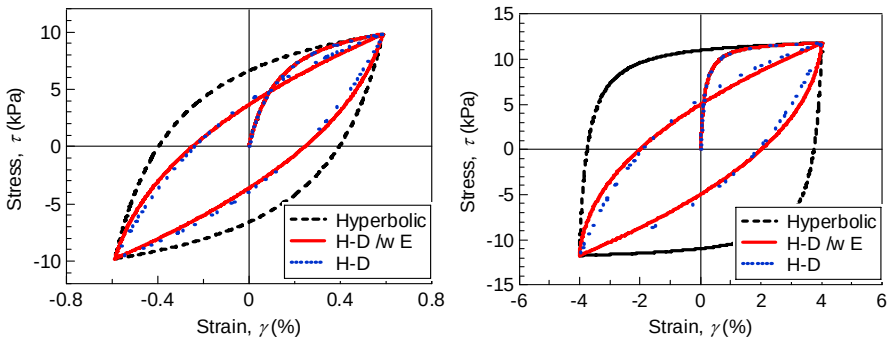

Figure 5. Stress-strain curve of clay.

4.2 *Earthquake motions*

Two earthquake motions are chosen among the earthquake motions shown by Sato et al. (1998), which is shown in Figure 6. They have limited number of large amplitude wave and large number of large amplitude wave, and are called shock wave and vibration wave, respectively. Since difference of damping characteristics appears at large strains. Therefore, the waves are scaled so that peak acceleration becomes 8 m/s^2 at the outcrop base layer.

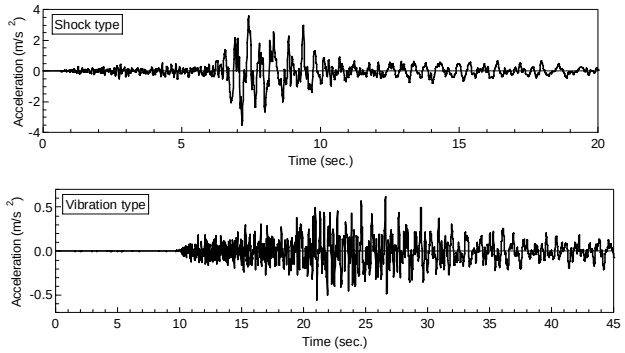

Figure 6. Earthquake motions to the engineering seismic base layer

4.3 *Response under shock wave and discussion*

Maximum response is shown in Figure 7. The maximum acceleration decreases rapidly at GL-5.8 m, resulting in about 2 m/s^2 at the ground surface. Since the layer between GL-3.8 and 5.8 m (clay layer) shows large strains of several percent, shear stress in these layer reaches shear strength, which can be confirmed through the chained line (shear strength) in Figure 7. If a layer reaches shear strength, acceleration above this layer reaches limit acceleration (Suetomi et al., 2000) because of the equilibrium condition of shear stress in this layer and inertia force above this layer. There is slight difference between hyperbolic model and H-D type model in the layer between GL-5.8 and 11.8 m; hyperbolic model shows larger acceleration. However, the difference is very small that we can say the response is identical in the engineering practice.

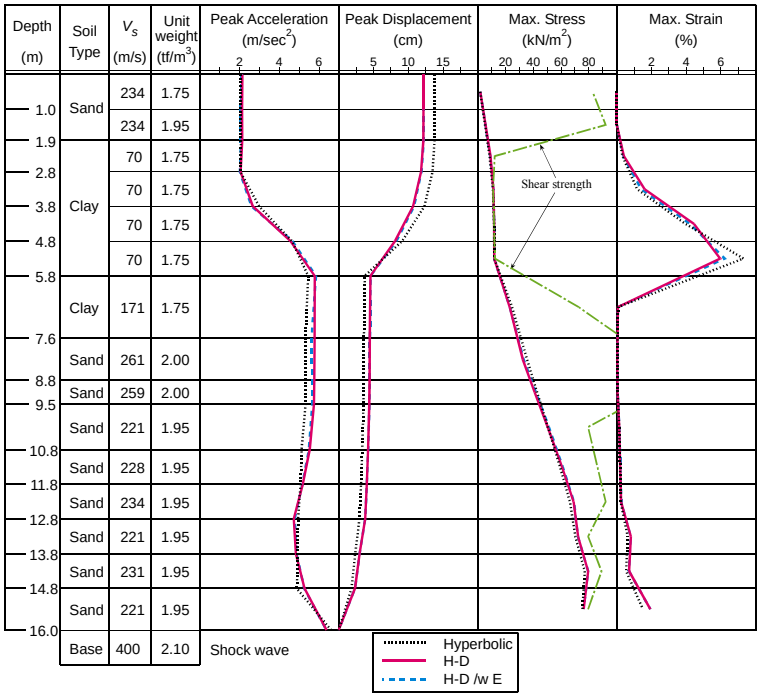

Figure 7. Maximum response under shock wave

Comparison of acceleration time history at the ground surface is shown in Figure 8. Although there is less difference in peak response, there are significant differences between hyperbolic model and H-D type model in the acceleration; hyperbolic model show large number of large acceleration wave whereas H-F type model shows small amplitude waves after the peak acceleration.

As discussed by Suetomi et al. (2000) and in the preceding, acceleration at the ground surface is strongly affected by the nonlinear behavior of the weakest layer. In order to see the differences more clear, stress-strain curve of the 6th layer where shear strength is the smallest and maximum shear strain is the largest is shown in Figure 9 and time history of strain is shown in Figure 10.

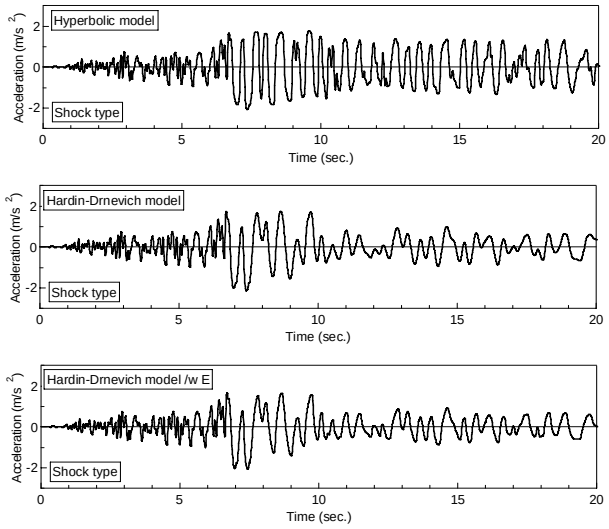

Figure 8. Acceleration time history at ground surface under shock wave

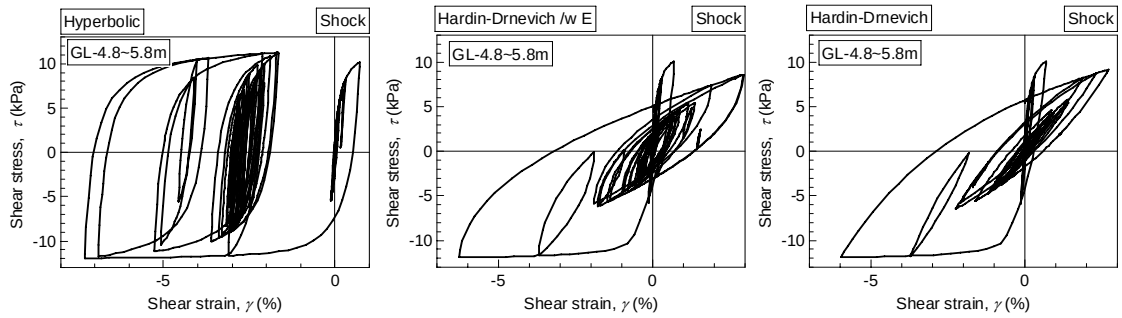

Figure 9. Stress-strain curves at 6th layer under shock wave

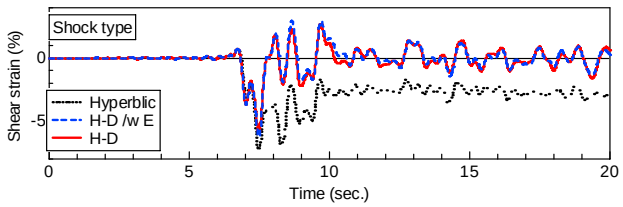

Figure 10. Stress-strain curve under shock wave

Maximum strain of several percents occurs at about 7.5 s following a relatively large spike at about 6.5 seconds with shear strain of about 1%. Shear strain is the largest in the hyperbolic model in both positive and negative sides. This is against the common sense that hysteresis curve with larger damping constant suppress the amplification resulting in smaller response (e. g., Railway Technical Research Institute, 1999). If, let suppose, earthquake motion is a mere pulse, the it is clear that only skeleton curve affects the maximum response and hysteresis loop does not affect it because maximum response occurs on the skeleton curve. Therefore, difference comes from the hysteretic behavior.

Since hyperbolic model has large damping, stiffness after unload becomes larger than H-D model, which can be seen clearly in Figure 5 and Figure 9. Therefore, shear stress increase more rapidly than that of H-D type model, which indicates that hyperbolic model keeps nearly perfect

state longer, resulting in large strains. On the other hand, since the stiffness is smaller after unload in the H-D type models, larger strain is required to cause the same shear stress as hyperbolic model. However, generating larger strain requires more time. If unload occurs before it, shear stress at the cycle becomes smaller. This seems the reason why H-D type models show smaller shear stress amplitude after maximum stress. This again explain why acceleration is smaller in H-D type models than that in hyperbolic model.

Finally acceleration response spectrum is shown in Figure 11. Acceleration is nearly identical in all models at period larger than 0.5 s, but that by hyperbolic model is much larger than that by H-D type models. This frequency range is important in the engineering practice. Therefore effect of shape of hysteresis loop is important in the earthquake response. It is also emphasized that model with larger damping ratio shows larger response acceleration.

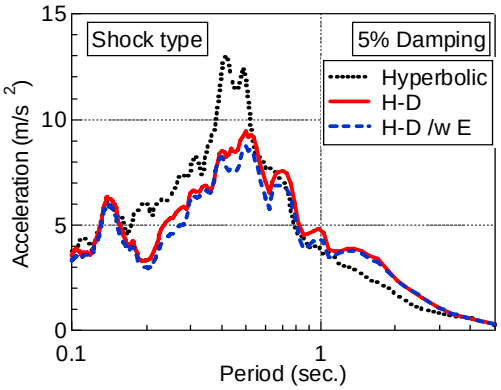

Figure 11. Response spectrum under shock wave

Differences between two H-D type models, that have same stiffness and damping characteristics but stiffness at unload is taken into account only in the proposed model in this paper, is not large; the behavior is quite similar. Regardless of the models, shape of the hysteresis loop must be in spindle shape. Therefore, if their area are same, then the possible shape is limited. Actually the shapes of both models is quite similar as can be seen in Figure 5 and Figure 9. This is the reason why two H-D type models show similar behavior.

4.4 *Response under vibration wave and discussion*

Same as shock wave case, maximum response is shown in Figure 12, acceleration time history at the ground surface is shown in Figure 13, stress-strain curves are shown in Figure 14, time history of shear strain is shown in Figure 15, and acceleration response spectrum is shown in Figure 16.

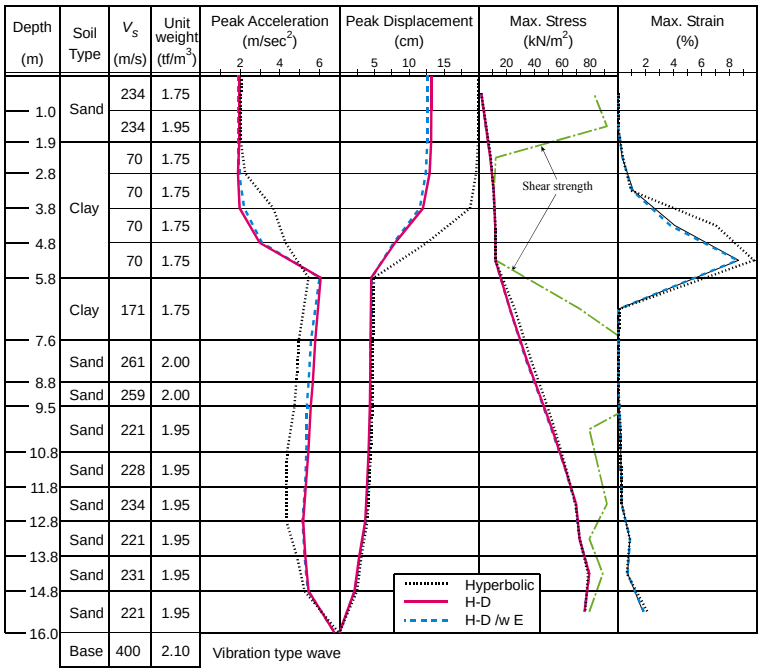

Figure 12. Maximum response under vibration wave

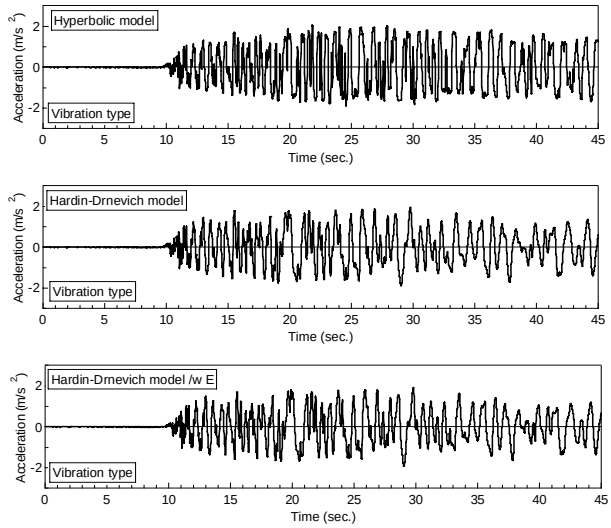

Figure 13. Acceleration time history at ground surface under vibration wave

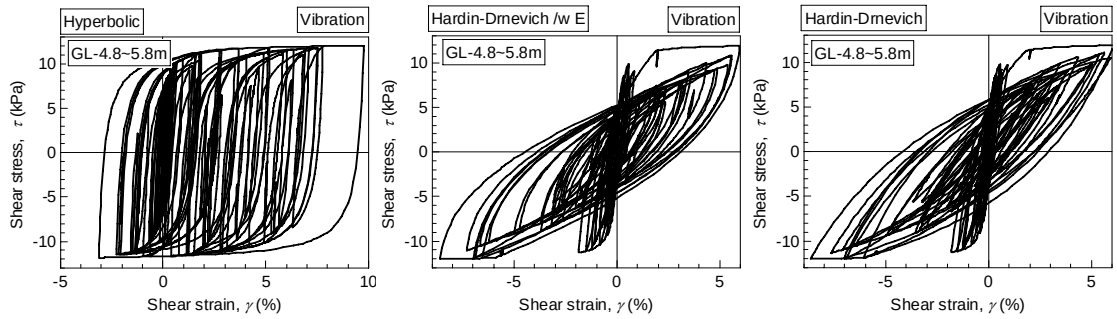

Figure 14. Stress-strain curve at 6th layer under vibration wave

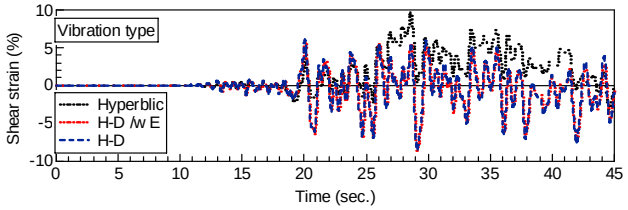

Figure 15. Strain time history at 6th layer under vibration wave

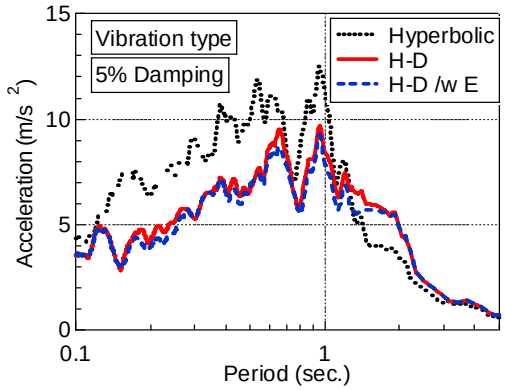

Figure 16. Response spectrum under vibration wave

5 CONCLUDING REMARKS

Stiffness at unload is shown not to be same as initial elastic modulus but depend on shear strain. Then a new constitutive model is proposed, which completely satisfy arbitrary given G-γ and h-γ relationships as well as stiffness at unload. Comparisons are made between the conventional hyperbolic model which shows much larger damping ratio than test and two H-D model type models both of which have the same strain dependent stiffness and damping characteristics and their damping characteristics follow the formula shown by Hardin and Drnevich (1972). In the two H-D models, the one uses hyperbolic model for hysteresis curve, where as the other uses R-O model in order to control stiffness at unload as well as strain dependent stiffness and damping characteristics. The following conclusions are obtained.

1) Stiffness at unload decreases with strain, and it can be modeled by a hyperbolic equation with minimum stiffness.

2) Difference of hysteresis loop does not affect the maximum response significantly under large earthquakes, because response at the ground surface is controlled by the shear strength of the weakest layer. On the other hand, they affect hysteretic behavior after unload. It affects response spectrum in shorter period, but affected period is important frequency for many structures.

3) It has been believed that response is smaller when damping constant is larger, but it is not true. If damping is larger, stiffness at unload becomes larger, which result in larger response at short period, but this period range is important in the engineering practice.

4) Effect to consider stiffness at unload is not large if damping characteristics is same, probably because shape of hysteresis loop essentially similar if area of the hysteresis loop is the same.

In conclusion, we should distinguish the effect of damping and maximum surface response which is strongly constrained by the shear strength at the weakest layer under large earthquakes. We also should recognize that larger damping creates larger stiffness after unload.

REFERENCES

Hardin, B. O. & Drnevich, V. P: 1972. Shear modulus and damping in soils: design equations and curves. *Proc. of the American Society of civil engineers*, 98 (SM7):.667-692

Ishihara, K., Yoshida, N. & Tsujino, S. 1985. Modelling of stress-strain relations of soils in cyclic loading, *Proc. 5th International Conference for Numerical Method in Geomechanics*, 1: 373-380

Iai, S., Matsunaga, Y. & Kameoka, T. 1999. Strain space plasticity model for cyclic mobility, *Soils and Foundations*. 32 (2): 1-15

Railway Technical Research Institute. 1999. Design standard of railway facilities and commentary, Maruzen, Tokyo

Yoshida, N., Tsujino, S. & Ishihara, K. 1990. Stress-strain model for nonlinear analysis of horizontally layered deposit, *Summaries of the Technical Papers of Annual Meeting of AIJ, Chugoku*. B (Structure I): 1639-1640 (in Japanese)

Takeshima, Y., Sawada, S., Fujii, N. & Yoshida, N. 2003. Effect of nonlinear modeling of hysteresis behavior on the dynamic response of ground, *Proc., 58th Annual Conf. of the JSCE*. I: 537-538 (in Japanese)

Sato, M., Yasuda, S., Yoshida, N. & Masuda, T. 1998. Simplified method for estimating maximum shear stress in the ground during earthquakes, *J. of Geotechnical Engineering, Proc. JSCE*. 610/III-45: 83-96 (in Japanese)

Suetomi, I., Sawada, S., Yoshida, N. and Toki, K. 2000. Relation between shear strength of soil and upper limit of earthquake ground motion, *J. of Structural Mechanics and Earthquake Engineering, Proc. JSCE*. 654/I-52: 195-206 (in Japanese)

Suetomi, I. and Yoshida, N. (1998): Nonlinear behavior of surface deposit during the 1995 Hyogoken-nambu earthquake, Soils and Foundations, Special Issue on Geotechnical Aspects of the January 17 1995 Hyogoken-Nambu earthquake, No. 2, pp. 11-22